

Development of two-phase flow downstream of a horizontal sudden expansion

Wael H. Ahmed, Chan Y. Ching ^{*}, Mamdouh Shoukri

Department of Mechanical Engineering, McMaster University, Hamilton, Ontario, Canada L8S 4L7

Received 13 December 2006; received in revised form 3 May 2007; accepted 11 June 2007

Available online 25 July 2007

Abstract

Experiments were performed to characterize the development of air–oil two-phase flow downstream of horizontal sudden expansions with area ratios of 0.0625 and 0.25. The tests were performed at oil and air superficial velocities in the range 0.02–0.756 and 0.136–3.75 m/s. In addition to the axial variation of the pressure and area-averaged void fraction, time-averaged local profiles of the void fraction, mean liquid velocity and turbulence intensity were measured downstream of the expansion using hot-film anemometry. The fully developed downstream void fraction can either increase or decrease from its upstream value, and depends on the flow pattern change across the expansion. The turbulence intensity is higher in the immediate vicinity of the sudden expansion. It then decreases with axial distance and asymptotes to an approximately constant value. The phase redistributions immediately downstream of the expansion and the developing length was found to be strongly dependent on the upstream flow pattern and the sudden expansion area ratio.

© 2007 Elsevier Inc. All rights reserved.

Keywords: Two-phase flow; Sudden area expansion; Developing length

1. Introduction

In most two-phase systems, different piping components such as sudden area changes, bends, valves and junctions are encountered. Reliable models to evaluate the local pressure losses as well as the effect of these components on the upstream and downstream flow characteristics are important to design such systems. While extensive research has been done on two-phase flow through straight pipes, there is only limited research on two-phase flow through different pipe singularities. The flow across sudden area expansions has been studied (Lottes, 1960; Mendler, 1963; Janssen and Kervinen, 1966; McGee, 1966; Attou and Bolle, 1997; Attou et al., 1997; Attou and Bolle, 1999), however, most of these efforts have been focussed on estimating the pressure recovery across the expansion. In a recent study, Ahmed (2005) showed that the pressure recovery was

dependent on both the wall shear stress in the developing region immediately downstream of the expansion and the wall pressure on the downstream face of the expansion. The phase redistribution in the developing region and the length of this region significantly affects these parameters. On the other hand, it was shown that once the flow developed fully, the flow pattern, void fraction and pressure gradient was characterized only by the pipe geometry and local flow conditions with no memory of its formation (Ahmed, 2005).

Several experimental investigations of two-phase flow across sudden expansions have been performed for vertical bubbly flow (Bel Fdhila et al., 1991; Rinne and Loth, 1996; Aloui et al., 1999), where local two-phase flow parameters such as void fraction, interfacial area concentration, bubble velocity, frequency and size have been measured. An attempt was made to incorporate interfacial transfer terms, such as the interfacial drag, according to the flow regime in the pressure recovery formulation (Attou et al., 1997; Schmidt and Friedel, 1996; Aloui and Souhar, 1996b), but the flow pattern transitions across the sudden expansion

^{*} Corresponding author. Tel.: +1 905 525 9140x24998; fax: +1 905 572 7944.

E-mail address: chingcy@mcmaster.ca (C.Y. Ching).

Nomenclature

<i>D</i>	downstream pipe diameter (m)
<i>d</i>	upstream pipe diameter (m)
<i>G</i>	mass flux ($\text{kg}/\text{m}^2 \text{s}$)
<i>J</i>	superficial velocity (m/s)
<i>L</i>	length (m)
<i>Re</i>	Reynolds number
<i>t</i>	time (s)
<i>u'</i>	turbulent velocity (m/s)
<i>U</i>	average liquid velocity (m/s)
<i>x</i>	mass quality of air ($\frac{G_G}{G_G+G_L}$)
<i>z</i>	axial direction (m)

<i>Greek symbol</i>	
σ	area ratio ($\frac{A_1}{A_2}$)

Subscripts

1	upstream of sudden expansion
2	downstream of sudden expansion
d	developing region
G	gas
L	liquid

section was not considered. There have been fewer experimental investigations of two-phase flow across horizontal sudden expansions. Aloui and Souhar (1996a) reported experimental data for bubbly flow over a horizontal flat plate with a sudden expansion as an application to plate heat exchangers. Their experimental results were characterized by a very small pressure recovery relative to the system pressure. The mass velocity of the liquid in this study was kept sufficiently high to avoid stratification and no change in the flow regime was observed during the dispersed bubbly flow.

Typically, the change in void fraction and the pressure recovery are used to characterize the flow across sudden area expansions. However, the redistribution of the two phases in the developing region and the developing length downstream of the sudden expansion are important to obtain more reliable flow models of the two-phase flow across sudden expansions. McGee (1966) reported a change from slug flow to churn flow and from churn to annular flow in a vertical sudden area expansion; however, no data were reported for these specific cases. Yang et al. (2001) and Ahmed et al. (2001) reported a variety of flow pattern changes across sudden area expansions and contractions based on observations and optical fibre probe signals. They concluded that the sudden expansion had a considerable effect on the phase redistribution immediately downstream of the expansion.

The objective of this work was to investigate the development of two-phase flow downstream of a sudden expansion. In particular, the change in the local void fraction and liquid velocity and turbulence structure in the developing region was characterized using hot-film anemometry. The developing length was estimated from these measurements and the phase redistribution downstream of the expansion was visualized using a high-speed camera. The experiments were performed for two area ratios of 0.0625 and 0.25 under different flow conditions. The experimental facilities are described in the next section, followed by a discussion of the phase redistribution in the developing region. The axial variation in the area-averaged void fraction and pres-

sure are presented next. Finally, the local measurements are presented along with the conclusions of this study.

2. Experimental facilities

The experiments were performed in an air–oil two-phase flow loop shown schematically in Fig. 1. The facility operates at pressures up to 415 kPa, with maximum air and oil flow rates of 43 kg/h and 1840 kg/h, respectively. Oil is supplied from a reservoir through a rotary gear pump that is controlled through a programmable speed controller. Air is taken from the main laboratory air supply at approximately 4 bar and regulated to the desired pressure through a pressure regulator. The air and oil are then mixed through an annular mixer. The oil flows on the outside of an inner perforated pipe, while the air flows in the inner pipe and enters the oil stream through 380 holes of 0.79 mm diameter. The air–oil mixture then passes through the horizontal test section, which has a total length of 3.5 m. Two area expansion ratios of approximately 0.0625 and 0.25 were used in this study. The test sections were made of commercially available clear polycarbonate tubing to allow for flow visualization. The two area ratios were obtained using 6.35 and 12.7 mm (0.25 and 0.5 in.) diameter tubing for the upstream section with 25.4 mm (1 in.) diameter tubing for the downstream section. The upstream and downstream lengths were 1.11 m and 2.5 m, respectively. The flow was visualized using a high-speed video camera that can operate at speeds up to 1000 frames/s.

The pressure distribution along the upstream and downstream sections was measured using a total of 18 pressure taps that were distributed along the upstream and downstream sections. The pressure distribution was measured using two differential pressure transducers, one absolute pressure transducer and two 12 channel pressure switching units. The absolute pressure transducer was connected to the first pressure tap along the test section which was used as a reference, while the differential pressure transducers were used to measure the pressure difference between the

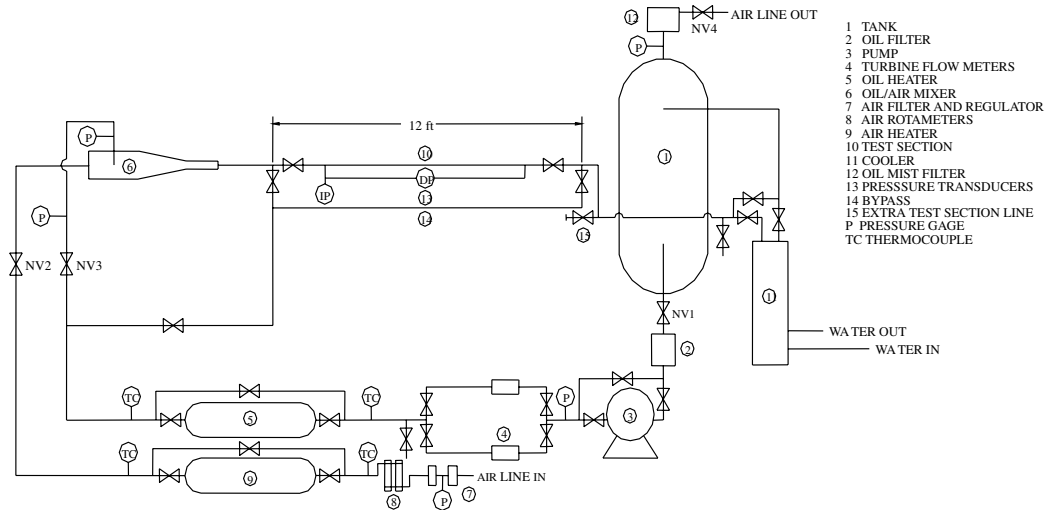


Fig. 1. Schematic diagram of air–oil two-phase flow loop.

first pressure tap and the other pressure taps distributed along the test section. The upstream pressure taps were connected to the higher pressure range differential pressure transducer (0–248.6 kPa) with an accuracy of $\pm 0.5\%$, while the downstream pressure taps were connected to the low pressure range differential pressure transducer (0–35 kPa) with an accuracy of $\pm 0.25\%$ full scale.

The axial variation of the average void fraction was measured using 10 ring capacitance sensors located along the test section. Each sensor consists of two pairs of active electrodes made of 5 mm brass strips spaced 2 mm apart to increase the signal to noise ratio by amplifying the absolute value of the capacitance circuit. Two separate half hollow cylinders made of acrylic are used for housing the elec-

trodes, and the unit is shielded using a 0.5 mm thick grounded brass electrode to eliminate stray capacitance between any of the electrodes, circuit and the wires. The housing is sandwiched together over the test section pipe and fastened using acrylic screws to make sure the electrodes are firmly in contact with the tube surface. The measurement volume of the capacitance sensor (length = $1.65D$) is small compared to the tube length, and the void fraction can be assumed to represent the average void fraction at a section along the tube. More details of sensor design and calibration are described in [Ahmed \(2005\)](#).

The local void distribution and the liquid velocity and turbulence intensities were measured using hot-film anemometry. The measurements were performed using a

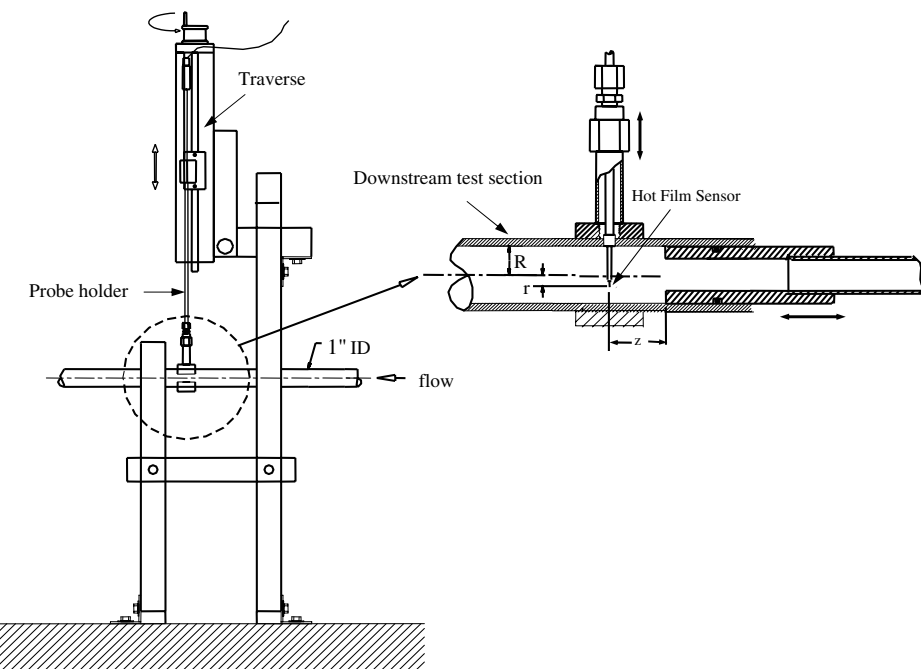


Fig. 2. Schematic diagram of test section with the hot-film set-up.

Table 1
Uncertainty in the measured and calculated quantities

Quantity	Uncertainty (%)
Pressure	±2–6%
Liquid mass flux	±2–10%
Mass quality	±3–4.5%
Local void fraction	±4–7%
Area-averaged void fraction	±3–5%
Local liquid velocity	±5–7%
Local void fraction	±5%

cylindrical TSI 1210-60W hot-film probe with a DISA 55M10 Constant Temperature Anemometry (CTA) bridge. The overheat ratio was set to 1.09, and is consistent with other reported hot-film anemometry measurements in

two-phase flow (Liu, 1989). A schematic diagram of the hot-film set-up is shown in Fig. 2. The hot-film is mounted on a traverse attached to the downstream test section which allows measurements at different radial positions with an accuracy of ±0.01 mm. The upstream test section is designed to be moved in the axial direction (Fig. 2) relative to the location of the hot-film probe in order to change the distance of the sensor from the sudden expansion. The hot-film signals were sampled at 5 kHz over a sampling period of 300 s which was found suitable to obtain statistically steady results. The highest frequency in the signal, determined from spectral tests, was found to be less than 1.5 kHz. The details of the hot-film calibration and the signal processing techniques are described by Ahmed (2005). The uncertainties of the measured and calculated quantities

Table 2
Fully developed upstream and downstream flow patterns for current flow conditions ($20 < G_{L1} < 2050 \text{ kg/m}^2 \text{ s}$)

Mass quality	Upstream flow pattern	Downstream flow pattern
$0.05 < x < 0$	Elongated bubble	Intermittent
	Intermittent flow	Elongated bubble
	Intermittent flow	Intermittent flow
	Intermittent flow	Stratified smooth/wavy flow
$x > 0.05$	Annular-mist flow	Annular-mist flow
	Annular-mist flow	Stratified wavy flow

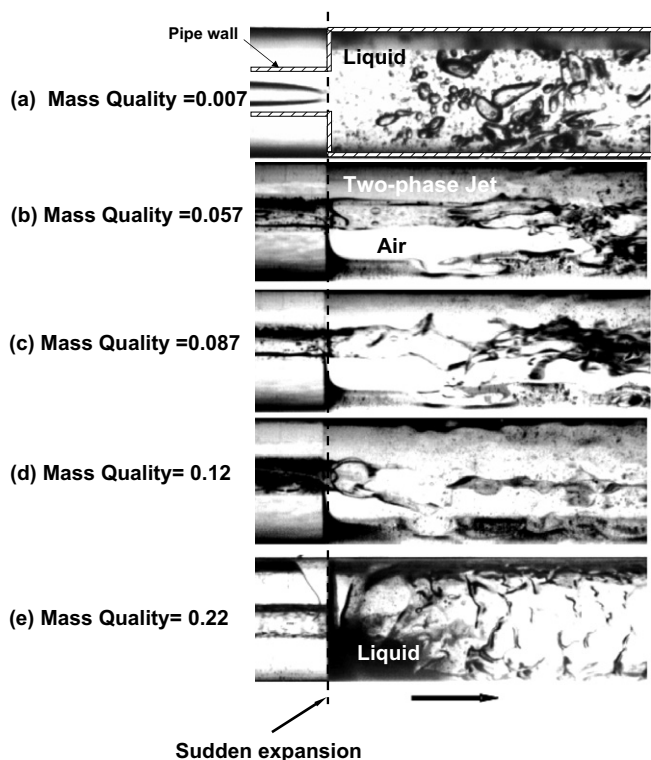


Fig. 3. Visualization of the phase redistribution immediately downstream of the sudden expansion with increasing mass quality for area ratio 0.0625 and $G_{L1} = 1050 \text{ kg/m}^2 \text{ s}$.

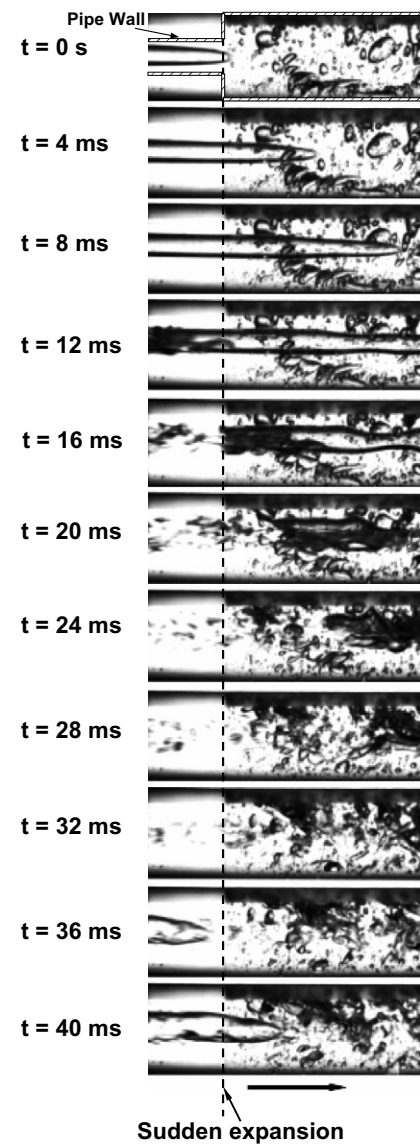


Fig. 4. Time sequence of images showing the phase redistribution downstream of the sudden expansion for an upstream plug flow for area ratio 0.25, $G_{L1} = 820 \text{ kg/m}^2 \text{ s}$ and $x = 0.001$.

were estimated using the method outlined by Moffat (1988), and are summarized in Table 1.

3. Results and discussion

3.1. Phase redistribution and flow pattern change

The phase redistribution in the developing region downstream of the sudden expansion plays an important role in determining the pressure on the downstream wall and the

additional wall shear stress in the developing region. The upstream flow patterns in the present study were elongated bubbly, intermittent (slug, plug and transition) and annular-mist, while the fully developed downstream flow patterns were elongated bubbly, intermittent, annular-mist and stratified wavy, and are summarized in Table 2.

Representative flow visualization images in the immediate vicinity of the sudden expansion for the 0.0625 area ratio with increasing mass quality are shown in Fig. 3. For an upstream plug flow, the flow transitions to bubbly

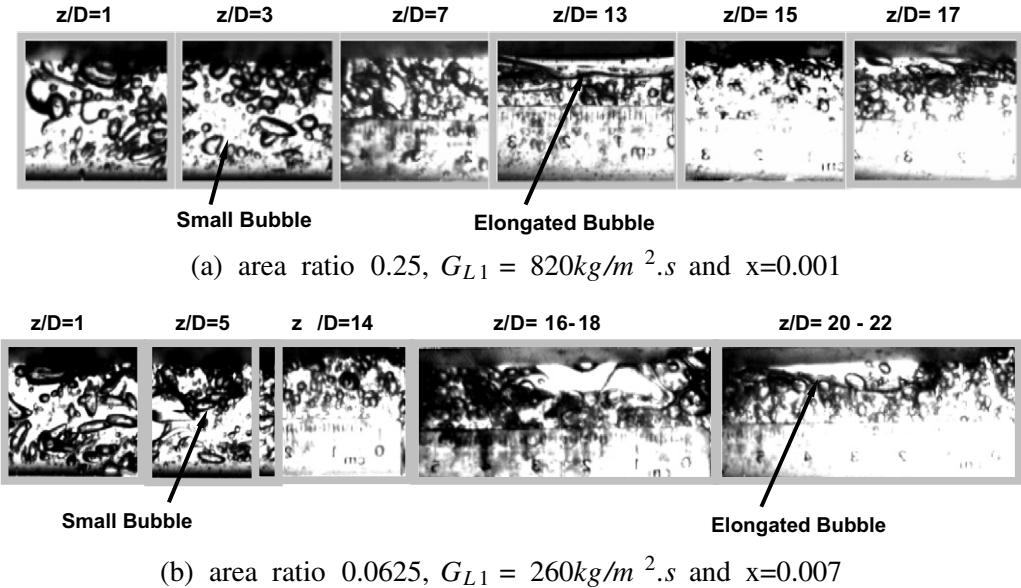


Fig. 5. Visualization of the development of the elongated bubbly flow downstream of the sudden expansion for (a) area ratio 0.25, $G_{L1} = 820 \text{ kg/m}^2 \cdot \text{s}$ and $x = 0.001$ and (b) area ratio 0.0625, $G_{L1} = 260 \text{ kg/m}^2 \cdot \text{s}$ and $x = 0.007$.

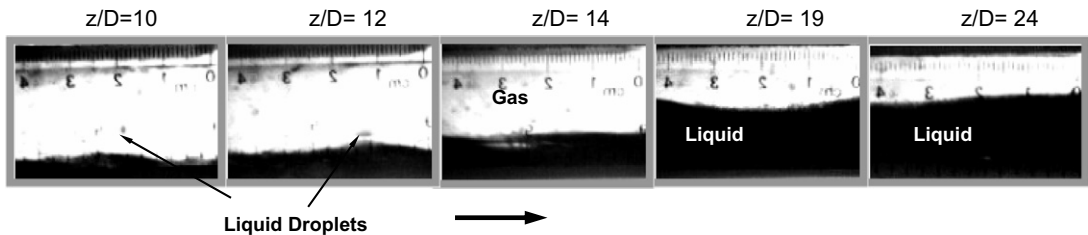


Fig. 6. Visualization of the development of the stratified wavy flow downstream of the sudden expansion for area ratio 0.0625 and $G_{L1} = 20 \text{ kg/m}^2 \cdot \text{s}$ and $x = 0.047$.

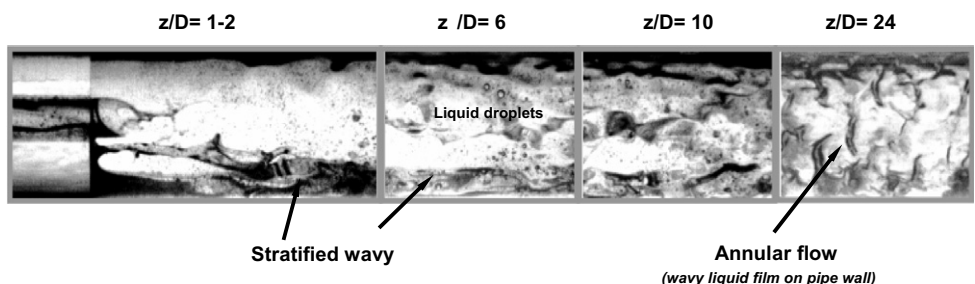
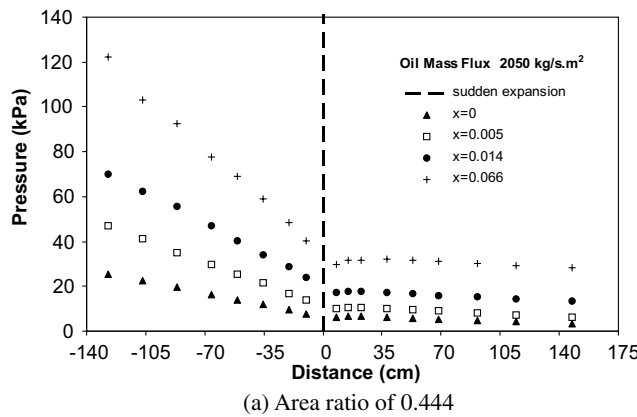
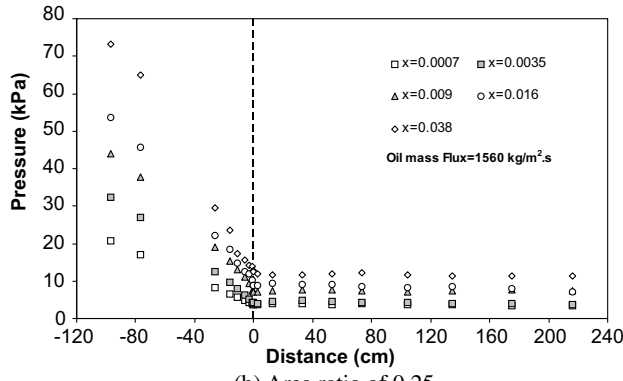


Fig. 7. Visualization of the development of the annular flow downstream of the sudden expansion for area ratio 0.0625 and $G_{L1} = 1050 \text{ kg/m}^2 \cdot \text{s}$ and $x = 0.12$.

flow downstream of the expansion as shown in Fig. 3a. In this case, as the gas plug enters the downstream section, it is subjected to a strong shear and results in a break-up of the gas plug into smaller voids. This is further illustrated in Fig. 4, where a sequence of images is shown over one cycle. These images show two interesting phenomena: (a) the deformation of the gas plug at $t = 12$ and 16 ms and (b) the break-up of the gas plug at $t = 20$ and 24 ms. The sequence is repeated with the approach of another gas plug at $t = 36$ ms. As the mass quality is increased, the upstream flow pattern becomes intermittent and finally annular. For the case of an annular upstream flow at mass quality of 0.057, the liquid film supports the gas core for a distance



(a) Area ratio of 0.444



(b) Area ratio of 0.25

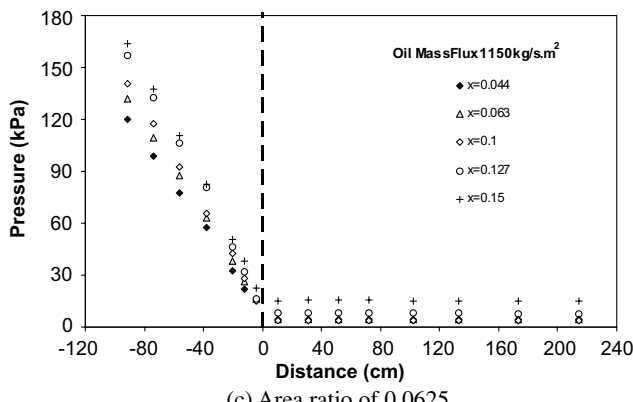
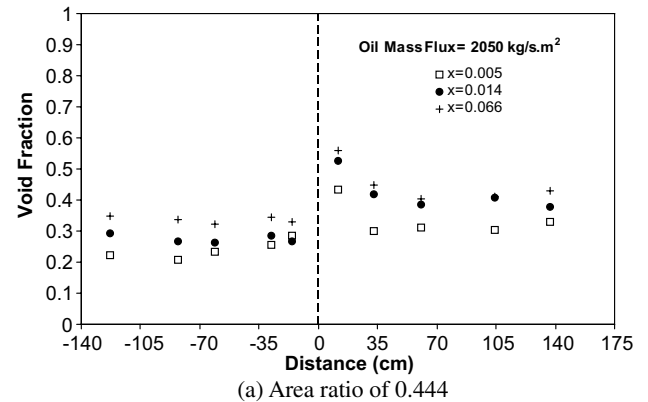
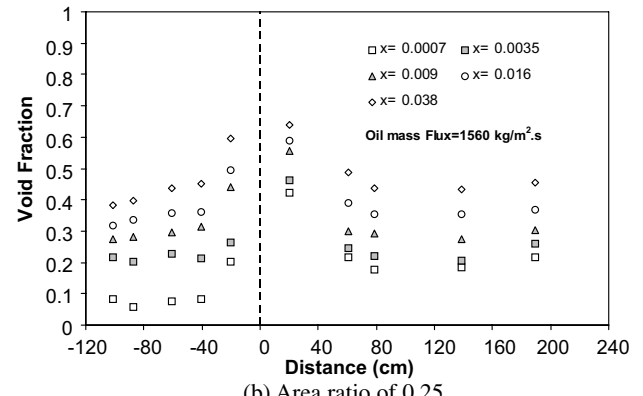


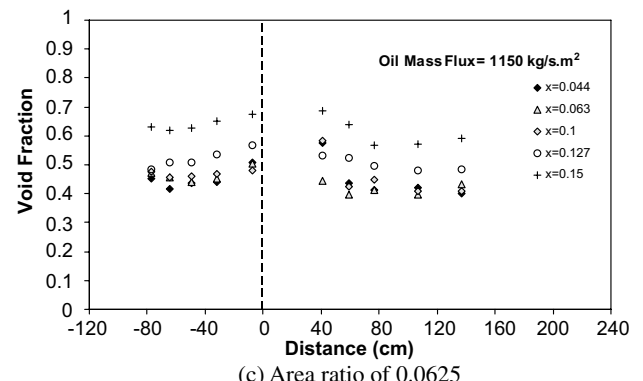
Fig. 8. Axial variation of pressure (gauge) across the sudden expansion for area ratio of (a) 0.444, (b) 0.25 and (c) 0.0625.



(a) Area ratio of 0.444



(b) Area ratio of 0.25



(c) Area ratio of 0.0625

Fig. 9. Axial variation of the average void fraction across the sudden expansion for area ratio of (a) 0.444, (b) 0.25 and (c) 0.0625.

of approximately two diameters downstream of the expansion, forming a two-phase jet flow as shown in Fig. 3b. This distance becomes shorter with increased quality, as the two-phase jet is subjected to higher shear stresses once it enters the larger tube that results in a more rapid distortion of the jet (Fig. 3c). At the higher mass qualities (0.12–0.22),

Table 3
Test conditions for local measurements of void fraction and liquid velocity

Area ratio	Downstream flow pattern	J_{L1} (m/s)	J_{G1} (m/s)
0.25	Elongated bubble flow	0.675	0.2
0.25	Elongated bubble flow	0.756	0.4
0.0625	Elongated bubble flow	0.27	0.2
0.0625	Stratified flow	0.02	3.75

the annular-mist flow bounded by the tube wall upstream is distorted immediately as the two-phase flow jet enters the downstream section (Fig. 3d and e).

The development of the elongated bubbly flow downstream of the sudden expansion is shown in Fig. 5 for the two area ratios. Images taken at different axial locations downstream of the expansion are shown in this figure. The bubbles tend to be distributed more uniformly immediately downstream of the sudden expansion due to the break-up and mixing of the upstream plugs as shown

above. This persists for a longer distance ($z/D \simeq 14$) for the 0.0625 area ratio compared to the 0.25 area ratio ($z/D \simeq 7$) due to the larger recirculation zone for the smaller area ratio. As the two-phase flow develops along the axial direction, the bubbles migrate to the upper part of the pipe due to buoyancy and coalesce. When the coalescence among the bubbles becomes significant, elongated bubbles are formed that ride on the upper part of the tube. This occurred at $z/D \simeq 10$ and $z/D \simeq 16$ for the area ratios 0.25 and 0.0625, respectively. As the quality is increased,

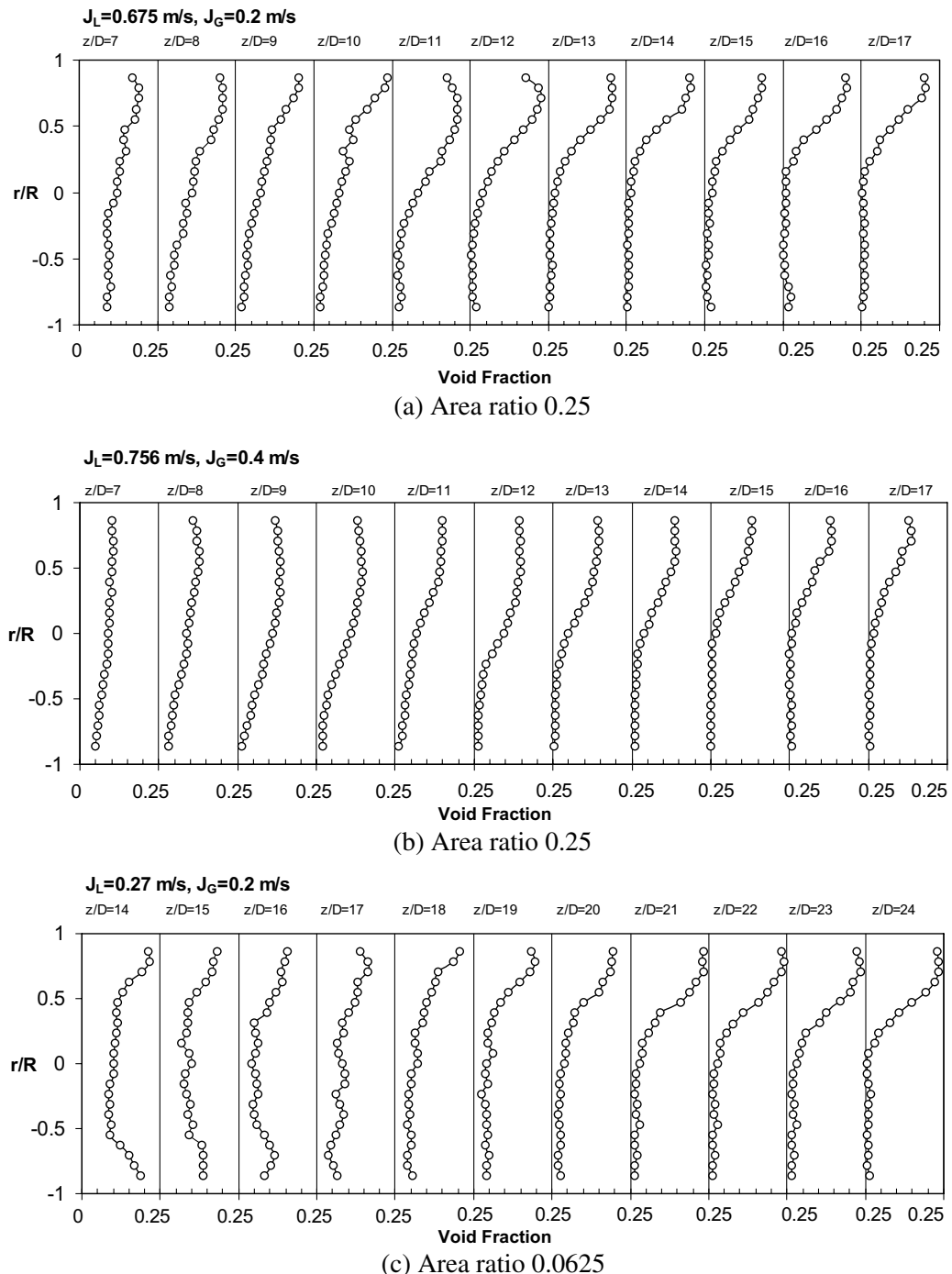


Fig. 10. Variation of the time-averaged local void fraction profiles downstream of the sudden expansion for elongated bubbly flow.

the upstream flow regime becomes annular with the corresponding fully developed downstream flow regime either wavy stratified or annular. The development of the wavy stratified flow downstream of the sudden expansion is shown in Fig. 6. The height of the liquid level increases with downstream distance, indicating a significant deceleration of the liquid phase under the adverse pressure gradient immediately downstream of the expansion. The gas velocity increases relative to the liquid velocity, with a consequent increase in slip and decrease in void fraction. The case with fully developed annular flow both upstream and downstream are shown in Fig. 7. As the annular

upstream flow enters the larger tube, the liquid strikes the tube wall and is drained into the lower part of the tube, which forms an initial wavy stratified flow. As the flow develops further, the wavy stratified flow can no longer be supported by the thinning liquid layer and the flow transition to annular flow.

3.2. Development of pressure and average void fraction

Representative axial pressure distributions across the sudden expansion for the different area ratios are shown in Fig. 8a–c. Additional data with an area ratio of 0.444 is

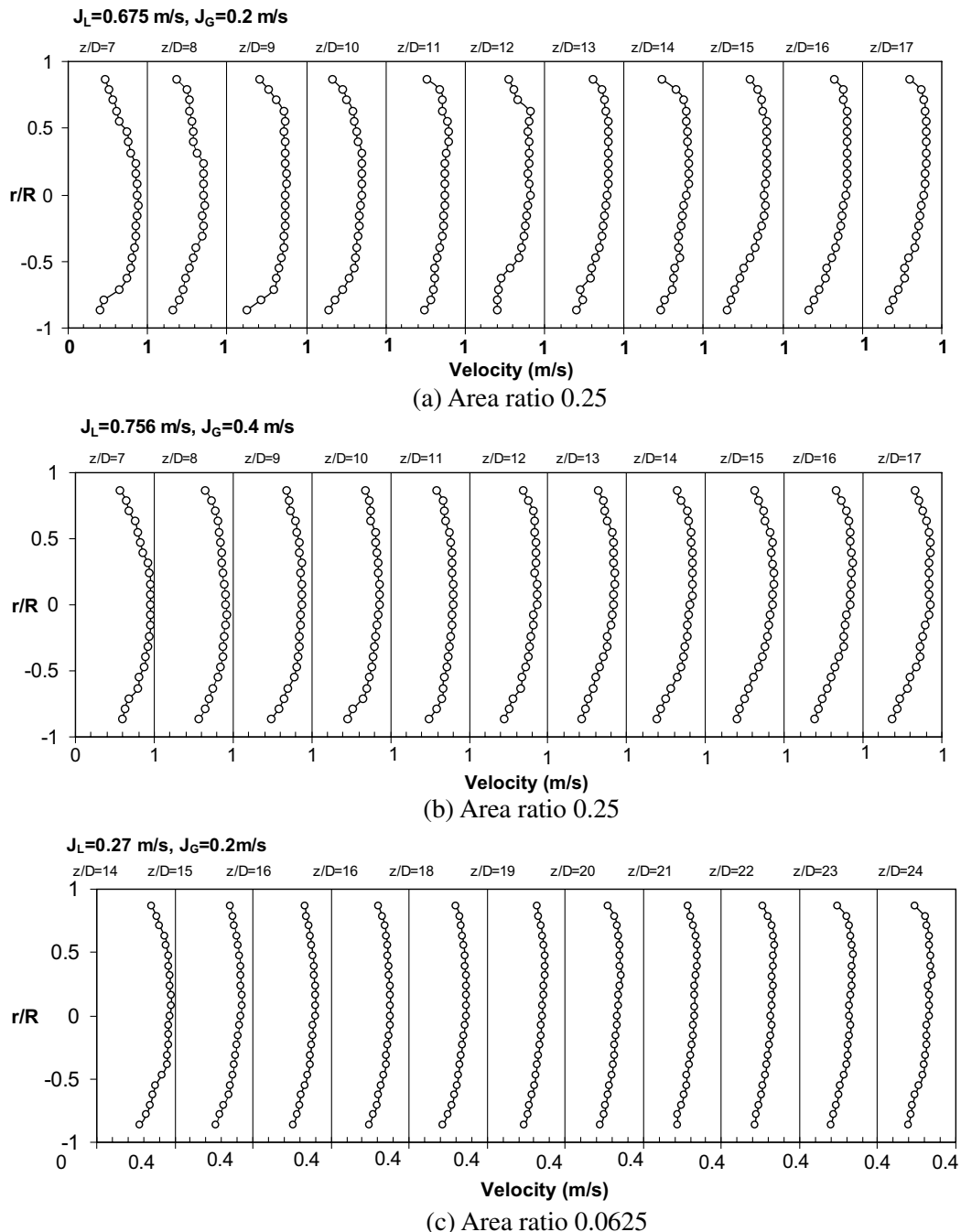


Fig. 11. Variation of the liquid velocity profiles downstream from the sudden expansion for elongated bubbly flow.

included in this figure. As expected, the pressure gradient upstream of the expansion increases as the quality increases because of the increase in liquid velocity and consequent increase in the friction losses. The minimum pressure is seen to occur a short distance downstream of the expansion due to the Vena Contracta effect. This is especially evident for the higher mass quality flows. The pressure then increases due to the area increase and deceleration of both phases, followed by the decrease due to pipe friction. The pressure gradient in the downstream section is significantly smaller than the upstream section due to the larger cross-sectional area.

The corresponding area-averaged void fraction profiles are shown in Fig. 9a–c. The void fraction increases as the flow approaches the sudden expansion, which is most discernible at the higher qualities. This is because the flow slows down under the influence of the adverse pressure gradient downstream of the sudden expansion. The gas phase is more affected by the adverse pressure gradient due to its lower axial momentum, and slows down more significantly than the liquid phase, resulting in an increase in void fraction. There is an increase in the void fraction immediately downstream of the expansion, which is most prominent for

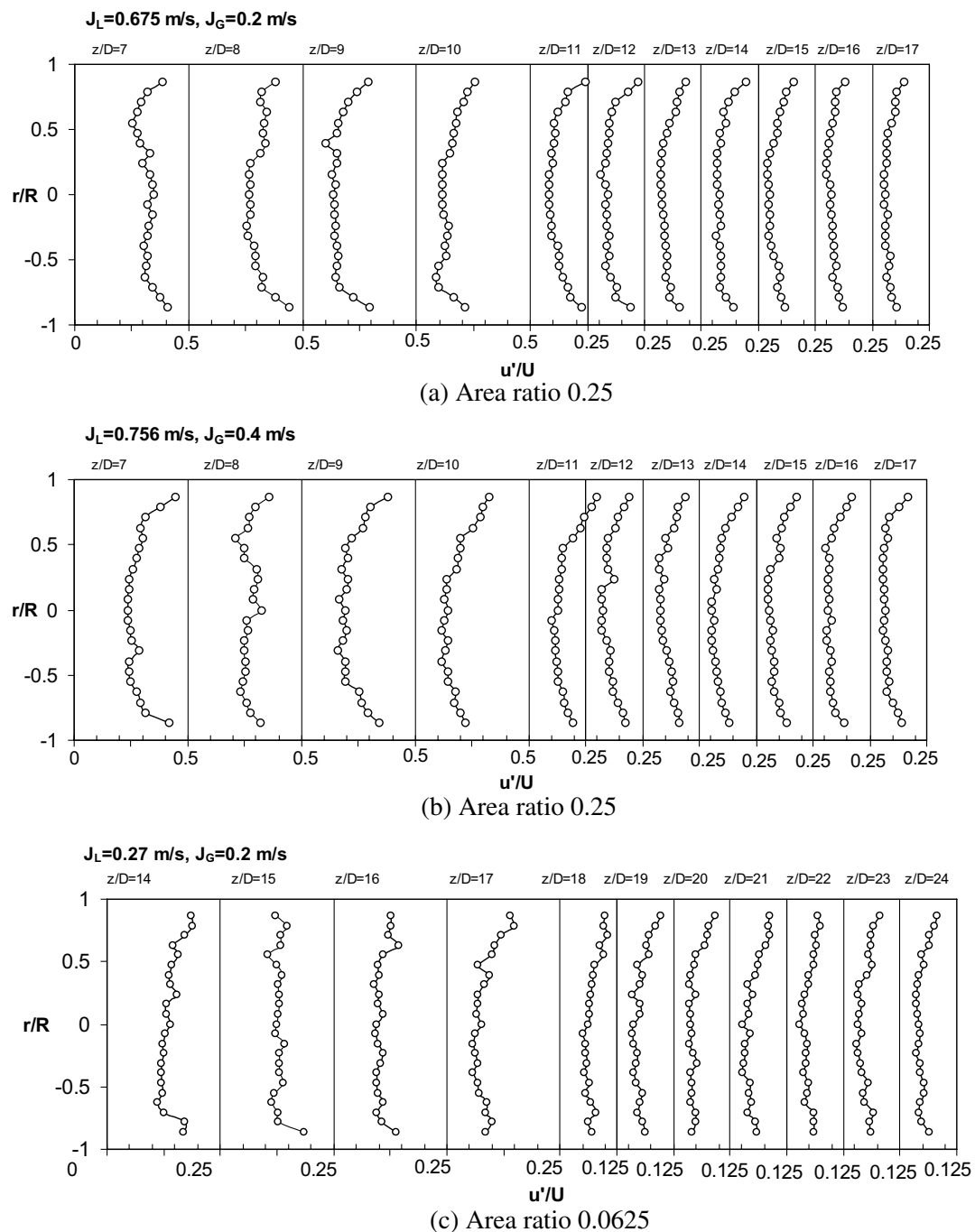


Fig. 12. Variation of the turbulence intensity profiles downstream of the sudden expansion for elongated bubbly flow.

the 0.444 area ratio. For example, in this case, at an oil mass flux of $2050 \text{ kg/m}^2 \text{ s}$ and quality of 0.014, the void fraction increases from a value of about 0.27 far upstream to about 0.52 at the closest downstream measurement location (10.7 cm) to the sudden expansion section (Fig. 9a). The increase is followed by a gradual decrease to approximately a constant value of 0.42, with the relaxation complete at about 30 cm (45D) downstream of the expansion. The sudden increase in void fraction immediately downstream of the sudden expansion is likely due to gas recirculation in the vicinity of the sudden expansion as observed in the flow visualizations, with the gas phase occupying a larger portion of this zone. This is plausible, as the liquid with a higher inertia will tend to follow the main streamline flow direction, rather than the recirculatory streamlines of the gas phase. At different mass qualities, the fully developed downstream void fraction can either decrease or increase from its upstream value. The fully developed values were estimated by averaging the void fraction values in the upstream and downstream sections where it was nearly constant. For example, for the area ratio of 0.25 and mass quality of 0.0007, the fully developed void fraction downstream is higher than the upstream value (Fig. 9b). In this case, the flow pattern changes from elongated bubble upstream to intermittent (slug) flow downstream of the sudden area expansion. The difference between the upstream and downstream values of the void fraction becomes smaller as the mass quality increases to 0.038 where intermittent flows are observed both upstream and downstream of the sudden expansion.

3.3. Local void fraction and liquid velocity and turbulence intensity profiles

The wall shear stress in the developing region downstream of a sudden expansion contributes significantly to the pressure recovery (Attou et al., 1997; Aloui et al., 1999). Hence, it is important to understand how the flow relaxes downstream of the sudden expansion. The development of the two-phase flow downstream of the sudden expansion was quantified here by the local void fraction, liquid velocity and liquid turbulence intensity profiles. Representative data for the local measurements with elongated bubbly flow and stratified flow in the fully developed region are presented in this section. The flow conditions for these measurements are given in Table 3.

The time-averaged void fraction profiles for the case with fully developed elongated bubbly flow are shown in Fig. 10a–c. Here, r/R represents the non-dimensional distance along the vertical axis from the pipe centerline. The value of $r/R = 1$ and $r/R = -1$ identifies the top and bottom of the pipe. The void fraction profiles are more uniformly distributed closer to the expansion, and develops into profiles that are higher in the upper half and nearly zero in the lower half. This is consistent with the flow visualizations presented in Fig. 5, where the liquid layer at the bottom of the pipe is nearly devoid of bubbles. The higher

void fraction in the top half reflects the larger bubbles present in this region. The profiles are fully developed at approximately $z/D = 14$ and $z/D = 21$ for the area ratios of 0.25 and 0.0625, respectively. The axial location where the two-phase flow is fully developed is defined here when the root mean square of the deviation between two consecutive profiles is less than 5%.

The corresponding time-averaged liquid velocity and turbulence intensity profiles are presented in Fig. 11a–c and Fig. 12a–c. The liquid velocity profiles in the fully developed region can be divided into two regions: (a) the lower part of the pipe where the void fraction is approximately zero, and (b) the upper part where the larger

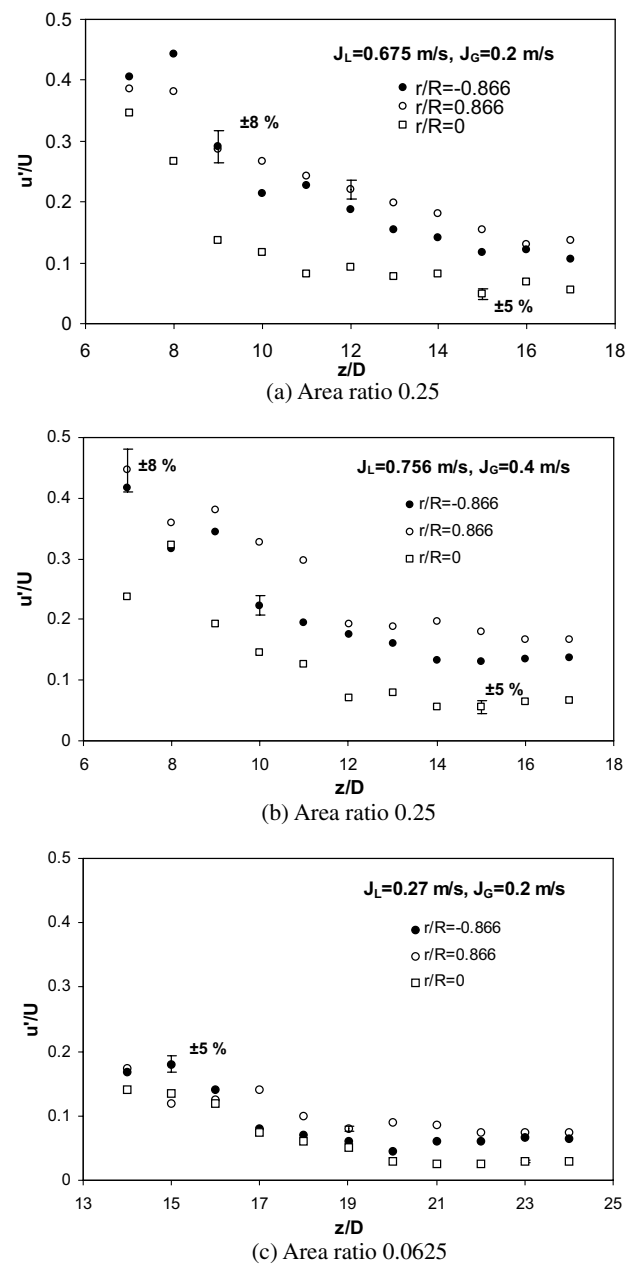


Fig. 13. Variation of the turbulence intensity downstream of the sudden expansion at different radial locations for elongated bubbly flow.

bubbles exist. The velocity is higher in the upper part of the pipe, reflecting the effect of the bubbles on the liquid velocity. Similar fully developed velocity profiles were obtained by Lewis and Kojasoy (2002) for slug flow in horizontal pipes. The turbulence intensity is higher in the immediate vicinity of the expansion due to the strong mixing as a result of the recirculation downstream of the sudden expansion. It should be noted, however, that the turbulence

intensity data may also include flow unsteadiness due to the mixing and recirculation. A spectral analysis is required if more details on the turbulence structure is required. This was not possible in this instance due to the highly intermittent nature of the liquid velocity signal due to the presence of the gas phase. As the distribution of the bubbles changes downstream of the sudden expansion, the turbulence intensity changes accordingly. The axial variation of the

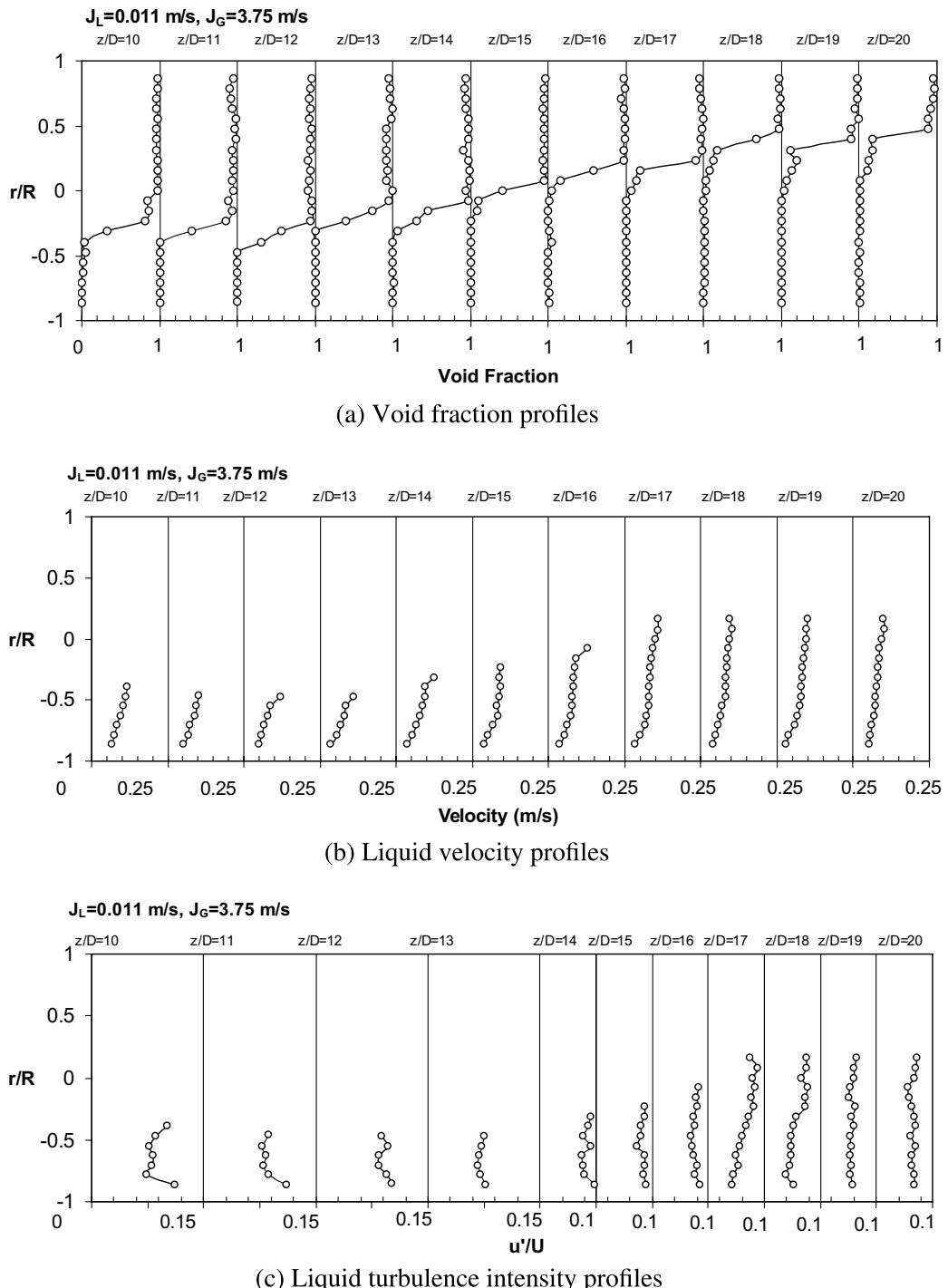


Fig. 14. Variation of the local (a) void fraction, (b) liquid velocity and (c) liquid turbulence intensity profiles for stratified wavy flow downstream of the sudden expansion with area ratio 0.0625.

turbulence intensity at three different radial locations ($r/R = +0.866, 0.0$ and -0.866) is shown in Fig. 13a–c. As the flow develops, the turbulence intensity decreases and asymptotes to approximately a constant value in the fully developed region. For example, for the 0.25 area ratio (Fig. 13a–b), at $r/R = 0.866$, the turbulence intensity decreases from about 40% at $z/D = 7$ to about 12% for $J_L = 0.675$ m/s and $J_G = 0.2$ m/s and to about 18% for $J_L = 0.756$ m/s and $J_G = 0.4$ m/s. For the area ratio of 0.0625, the turbulence intensity decreases from about 17% at $z/D = 14$ to about 5% for $J_L = 0.27$ m/s and $J_G = 0.2$ m/s (Fig. 13c). Typically, the turbulence intensity in the upper part of the pipe is higher than in the lower part. The higher turbulence intensities in the upper part can be attributed to the bubbles which are present in this region, which can increase the turbulence intensity.

The void fraction, liquid velocity and turbulence intensity profiles for the stratified wavy flow (area ratio 0.0625, $J_L = 0.011$ m/s and $J_G = 3.75$ m/s) are presented in Fig. 14. The void fraction profiles show a clear demarcation between the bottom liquid and upper gas layers (Fig. 14a). Here, the void fraction increases sharply across the interface from zero in the liquid layer to approximately unity in the gas region. As the flow develops, the thickness of the liquid layer increases and is consistent with the flow visualizations (Fig. 6). The liquid velocity, as expected, increases from the wall to a maximum value near the gas–liquid interface (Fig. 14b). It should be noted that no reliable measurements of the liquid velocity of the entrained liquid droplets in the gas phase can be made. The turbulence intensity decreases as the flow develops downstream of the sudden expansion and reaches an approximately constant value in the fully developed region (Fig. 14c).

3.4. Developing length downstream of expansion

The influence of the liquid mass flux on the developing length was found to be much more significant than the gas mass flux. The developing length, non-dimensionalized

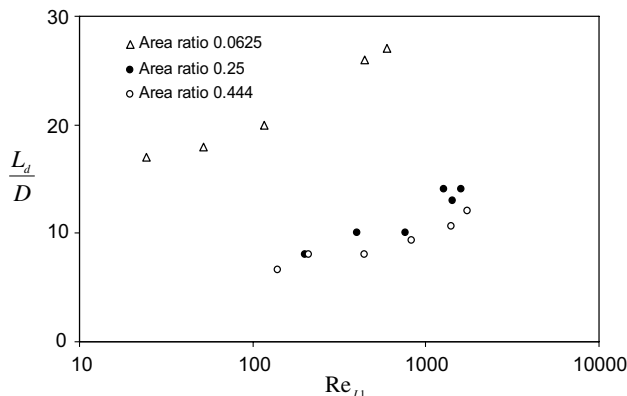


Fig. 15. Variation of the developing length with the upstream liquid Reynolds number.

by the pipe diameter, is plotted as a function of the upstream liquid Reynolds number, Re_{L1} , in Fig. 15 for the three area ratios. The developing length is defined here as the distance from the sudden expansion to the location where the root mean square deviation in the local void fraction profiles is less than 5%. It should be noted that the complete relaxation of the void fraction, liquid velocity and turbulence intensity downstream of the expansion does not occur at the same axial location. Typically, the void fraction relaxes first, followed by the liquid velocity and then the turbulence intensity. The developing length increases with both an increase in Re_{L1} and a decrease in the area ratio. With the constraint that the developing length approaches zero as σ approaches 1, the non-dimensional developing length can be correlated to the upstream liquid Reynolds number and area ratio using the current data as

$$\frac{L_d}{D} = 13.788 \cdot Re_{L1}^{0.11} (1 - \sigma)^{2.463} \quad (1)$$

for $\sigma \geq 0.0625$. This correlation, albeit a simplified one that does not consider the mass quality or the upstream flow regime, was found to fit the current data reasonably

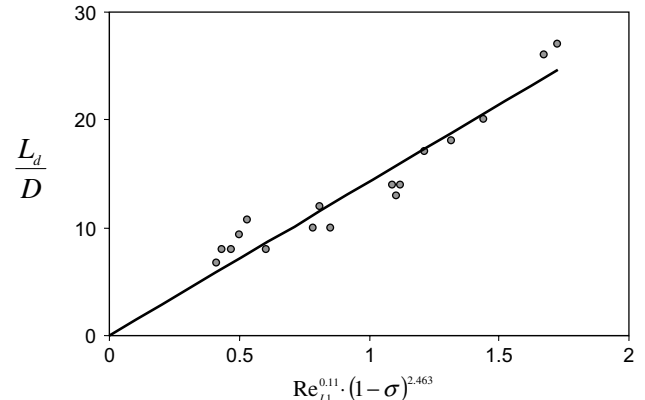


Fig. 16. Comparison of current data with the correlation for the developing length downstream of a sudden expansion.

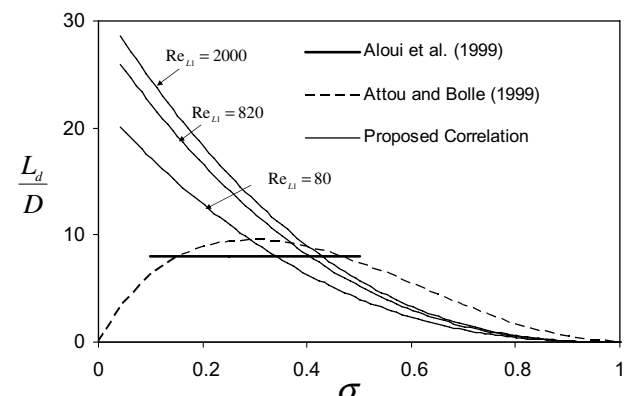


Fig. 17. Comparison of current correlation with existing correlations for the developing length downstream of a sudden expansion.

well with a correlation coefficient (R^2) of 0.84 as shown in Fig. 16, and can be considered to provide a first approximation for the developing length. The correlation developed in this study (Eq. (1)) is compared to that developed by Aloui et al. (1999) and Attou and Bolle (1997) in Fig. 17. Aloui et al. (1999) assumes a constant L_d/D that is independent of Reynolds number and area ratio, while Attou and Bolle (1997) takes into account the effect of area ratio, but not the liquid Reynolds number. The present correlation shows a more valid physical trend than the two previous correlations.

4. Conclusions

Experiments were performed to characterize the development of air–oil two-phase flow downstream of sudden expansions with area ratios of 0.0625 and 0.25. The axial variations of the pressure and area-averaged void fraction across the sudden expansion were obtained. In addition, the flow was visualized using a high-speed camera and the local void fraction, velocity and turbulence intensity profiles were measured downstream of the expansion using hot-film anemometry. The void fraction typically increases as the flow approaches the sudden expansion. The void fraction was also found to increase sharply across the expansion, followed by a relaxation to an approximately constant value in the fully developed region. The sudden increase in the void fraction immediately downstream of the expansion can be attributed to the separation of the gas from the two-phase flow in the recirculation region. The fully developed value of the void fraction downstream of the expansion can either increase or decrease from the upstream value, and depends on the flow pattern change across the expansion. The liquid turbulence intensity is higher in the immediate vicinity of the sudden expansion. It then reduces with axial distance and asymptotes to an approximately constant value in the fully developed region. The upstream flow pattern and area ratio was found to have a strong effect of the phase redistribution and the developing length downstream of the expansion. For the present test conditions, the void fraction profiles tend to develop faster than the liquid velocity and turbulent intensity profiles. The developing length was correlated to the area ratio and the upstream liquid Reynolds number.

Acknowledgements

The support of the National Sciences and Engineering Research Council (NSERC) of Canada and Pratt & Whitney Canada is gratefully acknowledged.

References

Ahmed, W.H., 2005. Two-phase flow through sudden area expansions. PhD Thesis, McMaster University, Hamilton, Ontario, Canada.

Ahmed, W.H., Ching, C.Y., Shoukri, M., 2001. Pressure recovery of air–oil two-phase flow across sudden expansions. In: CSME Forum, Kingston, Ontario, Canada, CD proceedings.

Aloui, F., Souhar, M., 1996a. Experimental study of a two-phase bubbly flow in a flat duct symmetric sudden expansion. Part II: Liquid and bubble velocities, bubble sizes. *Int. J. Multiphase Flow* 22 (5), 849–861.

Aloui, F., Souhar, M., 1996b. Experimental study of a two-phase bubbly flow in a flat duct symmetric sudden expansion. Part I: Visualization, pressure and void fraction. *Int. J. Multiphase Flow* 22 (4), 651–665.

Aloui, F., Doublez, L., Legarand, J., Souhar, M., 1999. Bubbly flow in an axisymmetric sudden expansion: pressure drop, void fraction, wall shear stress, bubble velocities and sizes. *Exp. Therm. Fluid Sci.* 19, 118–130.

Attou, A., Bolle, L., 1997. Integral formulation of balance equations for two-phase flow through a sudden enlargement. Part 1: Basic approach. *Proc. Inst. Mech. Eng. Part C*, 211.

Attou, A., Bolle, L., 1999. Theoretical analysis of the two-phase steady flow characteristics parameters of a sudden enlargement. *Z. Angew. Math. Phys.* 50, 731–758.

Attou, A., Giot, M., Seynhaeve, M., 1997. Modeling of steady-state two-phase bubbly flow through a sudden enlargement. *Int. J. Heat Mass Transfer* 40 (14), 3375–3385.

Bel Fdhila, R., Suzanne, C., Masbernat, L., 1991. Measurements in Two-Phase Bubbly Flows in Complex Geometries. In: Hewitt, G.F., Mayinger, F., Riznic, J.R. (Eds.), *Phase-Interface Phenomena In Multi-Phase Flow*. Hemisphere Publishing Corporation.

Janssen, E., Kervinen, J.A., 1966. Two-phase pressure drop across contractions and expansions of water-steam mixture at 600–1400 psia. In Report Geap 4622-1965-US.

Lewis, S., Kojasoy, G., 2002. Internal flow structure description of slug flow-pattern in horizontal pipe. *Int. J. Heat Mass Transfer* 45, 3897–3910.

Liu, T., 1989. Experimental investigation of turbulence structure in two-phase bubbly flow. PhD Thesis, Northwestern University, Illinois, USA.

Lottes, P.A., 1960. Expansion losses in two-phase flow. *Nucl. Sci. Eng.* 9, 26–31.

McGee, J.W., 1966. Two-phase flow through abrupt expansion and contraction, PhD Thesis, North Carolina State University at Raleigh.

Mendler, O.J., 1963. Sudden expansion losses in single and two-phase flow, PhD Thesis, University of Pittsburgh, Pennsylvania.

Moffat, R.J., 1988. Describing the uncertainties in experimental results. *Exp. Therm. Fluid Sci.* 1, 3–17.

Rinne, A., Loth, R., 1996. Development of local two-phase flow parameters for vertical bubbly flow in a pipe with sudden expansion. *Exp. Therm. Fluid Sci.* 13 (2), 152.

Schmidt, J., Friedel, L., 1996. Two-phase pressure change across sudden expansions in duct areas. *Chem. Eng. Commun.* 141, 175–190.

Yang, Y., Li, G., Zhou, F., Chen, X., 2001. Flow pattern and their transition characteristics of air–water two-phase flow in a horizontal pipe with sudden-changed cross section area. *Nucl. Sci. Tech.* 12 (1), 44–52.